Cell Metabolism, Volume *35*

Supplemental information

Hepatic levels of S-adenosylmethionine regulate the adaptive response to fasting

Alba Capelo-Diz, Sofía Lachiondo-Ortega, David Fernández-Ramos, Jorge Cañas-Martín, Naroa Goikoetxea-Usandizaga, Marina Serrano-Maciá, Maria J. González-Rellan, Laura Mosca, Joan Blazquez-Vicens, Alberto Tinahones-Ruano, Marcos F. Fondevila, Mason Buyan, Teresa C. Delgado, Virginia Gutierrez de Juan, Paula Ayuso-García, Alejandro Sánchez-Rueda, Sergio Velasco-Avilés, Héctor Fernández-Susavila, Cristina Riobello-Suárez, Bartlomiej Dziechciarz, Cristina Montiel-Duarte, Fernando Lopitz-Otsoa, Maider Bizkarguenaga, Jon Bilbao-García, Ganeko Bernardo-Seisdedos, Ana Senra, Mario Soriano-Navarro, Oscar Millet, Ángel Díaz-Lagares, Ana B. Crujeiras, Aida Bao-Caamano, Diana Cabrera, Sebastiaan van Liempd, Miguel Tamayo-Caro, Luigi Borzacchiello, Beatriz Gomez-Santos, Xabier Buqué, Diego Sáenz de Urturi, Francisco González-Romero, Jorge Simon, Rubén Rodríguez-Agudo, Asier Ruiz, Carlos Matute, Daniel Beiroa, Juan M. Falcon-Perez, Patricia Aspichueta, Juan Rodríguez-Cuesta, Marina Porcelli, María A. Pajares, Cristina Ameneiro, Miguel Fidalgo, Ana M. Aransay, Tomas Lama-Díaz, Miguel G. Blanco, Miguel López, Ricardo Villa-Bellosta, Timo D. Müller, Rubén Nogueiras, Ashwin Woodhoo, María Luz Martínez-Chantar, and Marta Varela-Rey

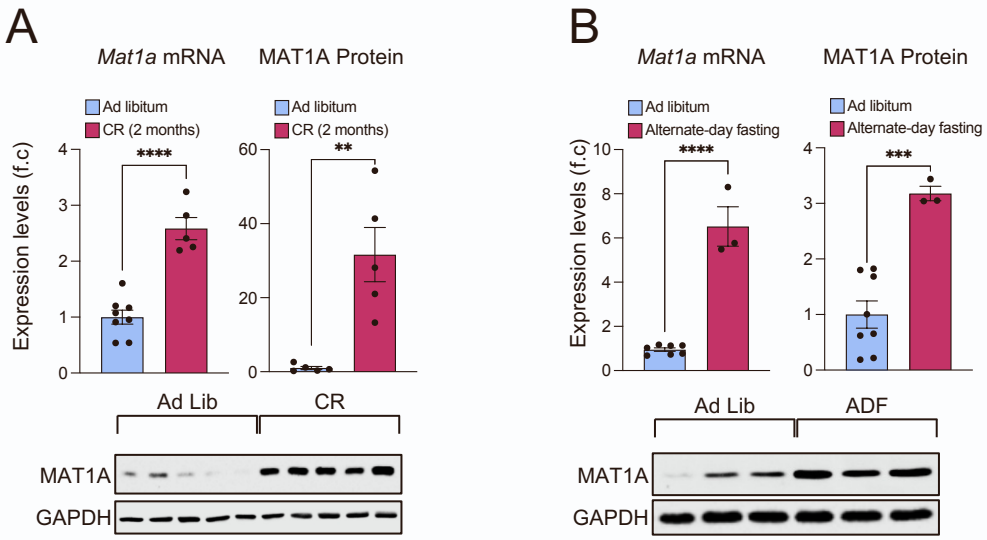

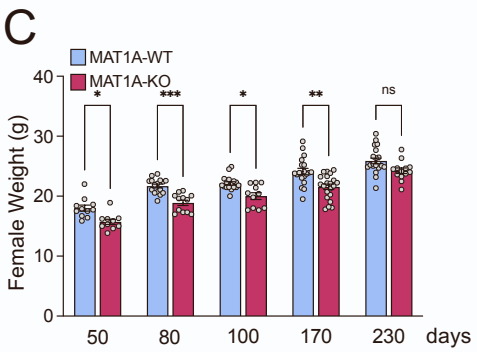

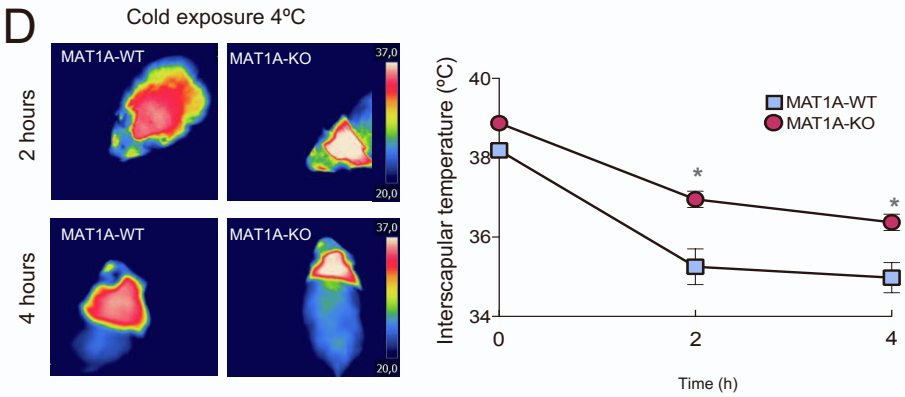

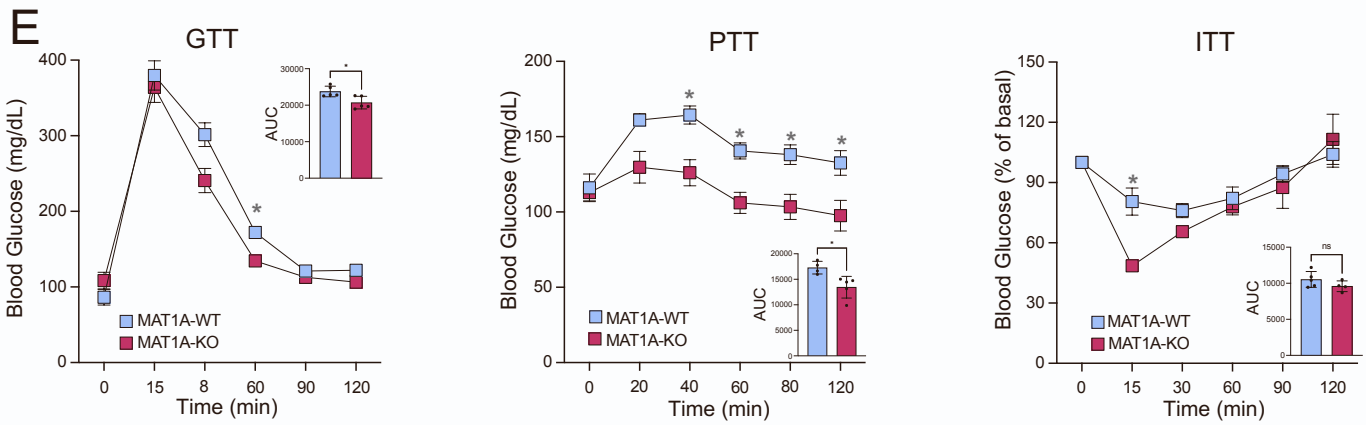

Supplemetary Figure 1

Figure S1. ***Fasting-induced MAT1A expression, enhanced energy expenditure and glucose, pyruvate and insulin tolerance in MAT1A-KO mice, related to Figure 1 and 2.***
(**A, B**) RT-qPCR and representative immunoblotting analyses show an increase in *Mat1a* mRNA and MAT1A protein expression after two months under (**A**) 40% of CR (n=5-8) or (**B**) ADF (n=3-7). Graph shows densitometric analysis of MAT1A protein from immunoblots. (**C**) Weight of female WT and MAT1A-KO mice fed ad libitum over a 230-day period (n=10-21). (**D**) Representative BAT thermographic picture and graph of interscapular temperatures of *ad libitum*-fed WT and MAT1A-KO male mice under cold exposure to 4ºC (n=4-5 per group). (**E**) Intraperitoneal glucose tolerance test (GTT), insulin tolerance test (ITT), and pyruvate tolerance test (PTT) in age-matched male MAT1A-WT and KO mice (n=4-5). Results are presented as mean ± SEM. *p<0.05, ** p<0.01 *** p<0.001 and **** p<0.0001 by two-way Anova (C, D, and E) or Student's *t*-test (A and B). f.c. denoted fold change.

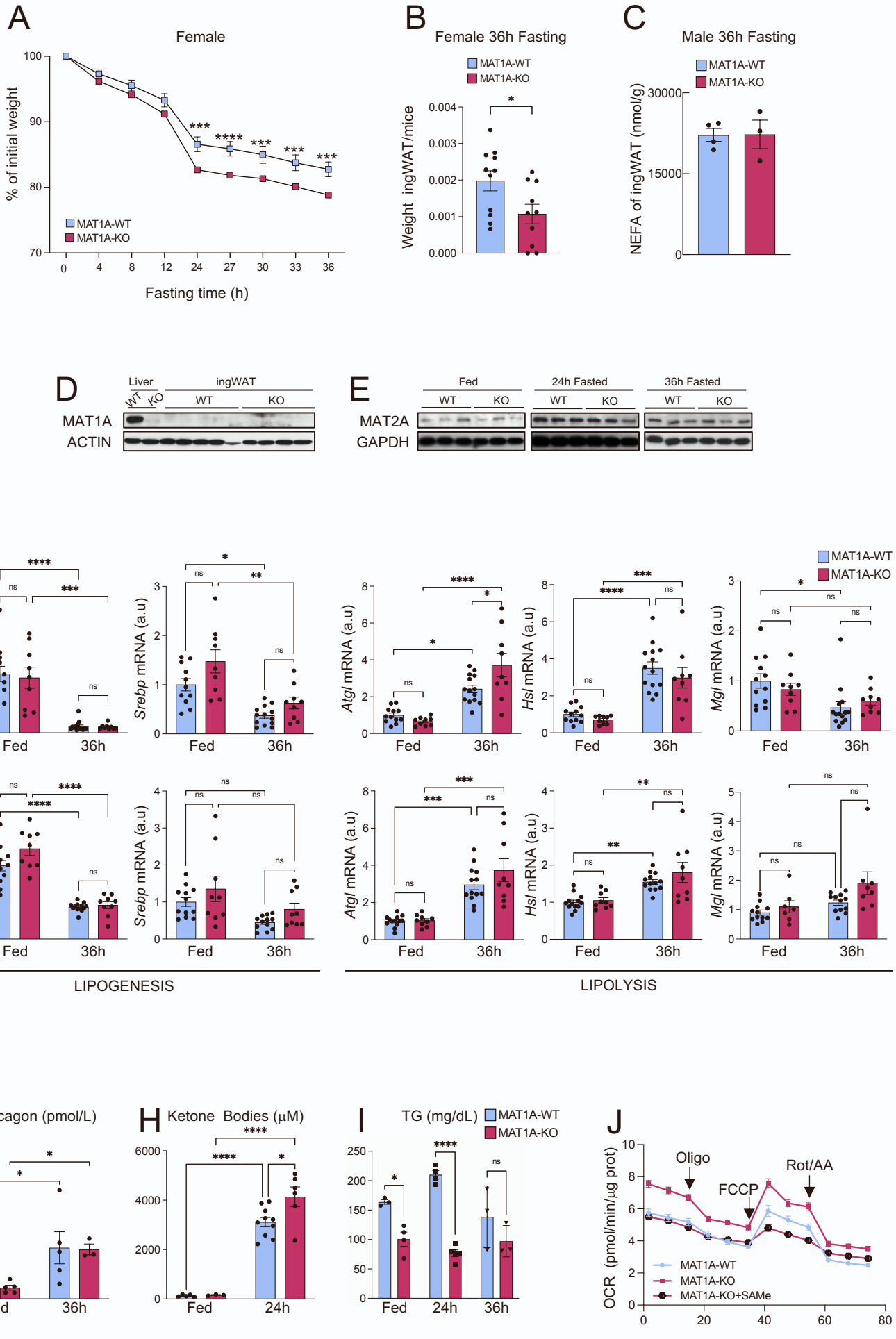

Supplemetary Figure 2

Figure S2. ***Phenotypic characteristics of male and female MAT1A-KO mice under fasting, related to Figure 3 and 4.***

(**A**) Graph showing more pronounced weight loss in female MAT1A-KO mice fasted over a 36h period (n=4-9). (**B**) Ratio of ingWAT/mice weights in 50-60 days old female MAT1A-KO mice fasted during 36h (n=10-11). (**C**) Lipolysis measured by NEFA released to the culture medium for 4h in explants of ingWAT from male WT and MAT1A-KO mice fasted over a 36h period (n=3-4). (**D**-**F**) Immunoblot analysis of (**D**) MAT1A protein expression in liver, and ingWAT from 24h fasted MAT1A-KO mice (n=4-5), and (**E**) MAT2A protein expression in BAT from fed and fasted MAT1A-KO mice (n=3-5). (**F**) RT-qPCR from ingWAT (upper panel, n=9-12) and BAT (lower panel, n=7-13)) of lipogenic genes (*Fas* and *Srebp*), and lipolytic genes (*Atgl*, *Hsl* and *Mgl*). (**G-I**) Graphs showing a (**G**) similar increase in serum glucagon levels (n=3-5) and (**H**) an enhanced increase in serum ketone bodies induced by fasting in MAT1A-KO mice compared to WT mice (n=3-10), and (**I**) a consistent decrease in serum TG levels (n=3-5) in MAT1A-KO mice both under fed conditions and after fasting. (**J**) Primary MAT1A-KO hepatocytes, obtained from 24h fasted mice, were treated with vehicle or 4mM SAMe for 4 hrs, and compared to untreated MAT1A-WT hepatocytes (n=6-8). Oligomycin (1μM), FCCP (1 μM), and rotenone (0.5 μM) combined with antimycin (0.5 μM) were added sequentially to hepatocytes and mitochondrial oxygen consumption rate (OCR) was measured. Results are presented as the mean ± SEM *p<0.05, ** p<0.01 and *** p<0.001 by two-way Anova (A, F-I) or Student's *t*-test (B and C).

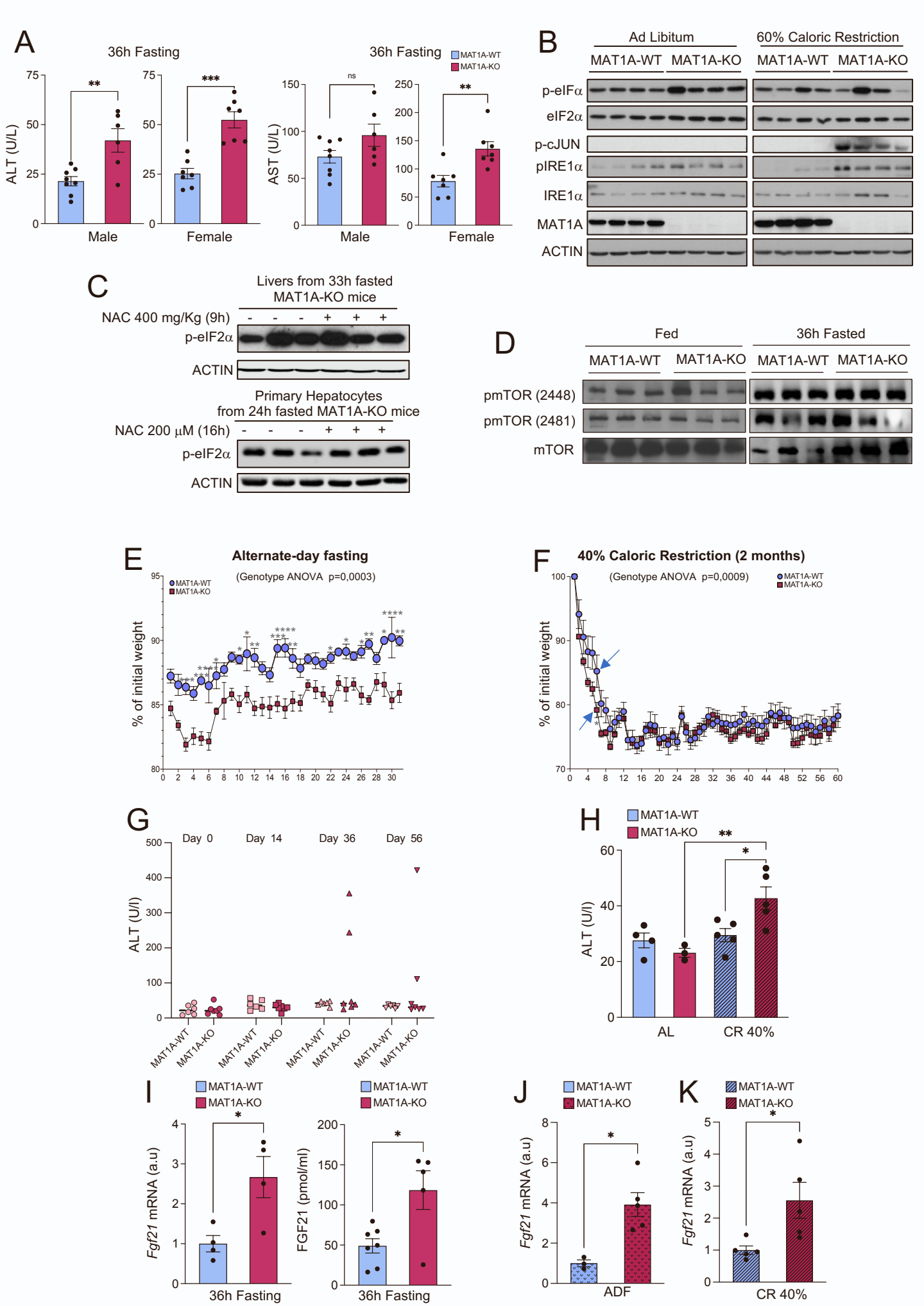

Supplemetary Figure 3

Figure S3. Impact of the absence of *MAT1A during fasting, ADF or CR, related to Figure 3 and 4.*

(**A**) Graphs showing an increase in serum transaminases (AST, ALT) in male and female MAT1A-KO mice after 36h of fasting (n=6-8). (**B**) Immunoblot analysis of proteins involved in ER stress and UPR in total liver extracts from MAT1A-WT and KO mice fed ad libitum or under 60 % of CR for 5 days (n=4). (**C**) NAC (400 mg/kg) was administered intravenously 9h before sacrifice in MAT1A-KO mice fasted during 36h and immunoblot analysis of p-eIF2α in total liver extracts was performed (*upper panel*) (n=3). MAT1A-KO primary hepatocytes were isolated from 24h fasted mice and were untreated or treated with 200μM NAC during 16h, followed by immunoblot analysis of p-eIF2α in total extracts (*bottom panel*). (**D**) Immunoblot analysis of mTOR phosphorylation in total liver extracts from MAT1A-WT and KO mice fed ad libitum or fasted during 36h (n=5-6). Percentage of weight loss of mice (**E-F**) fed during two months with (**E**) ADF (n=4-7) or (**F**) under a 40% of CR (n=4-5), and serum ALT levels in MAT1A-KO mice fed during two months with (**G**) ADF (n=6-7) or (**H**) under a 40% of CR (n=3-5). (**I**) Graphs showing elevated *Fgf21* mRNA (n=4) and serum FGF21 levels (n=5-7) in fasted MAT1A-KO female mice. Graphs showing elevated *Fgf21* mRNA levels in MAT1A-KO male mice fed during two moths with (**J**) ADF (n=3-5) or (**K**) 40% of CR (n=5). Results are presented as the mean $\pm$ SEM *p<0.05, ** p<0.01, *** p<0.001 and **** p<0.0001 by two-way Anova (D-G) or Student's *t*-test (A, H-J).

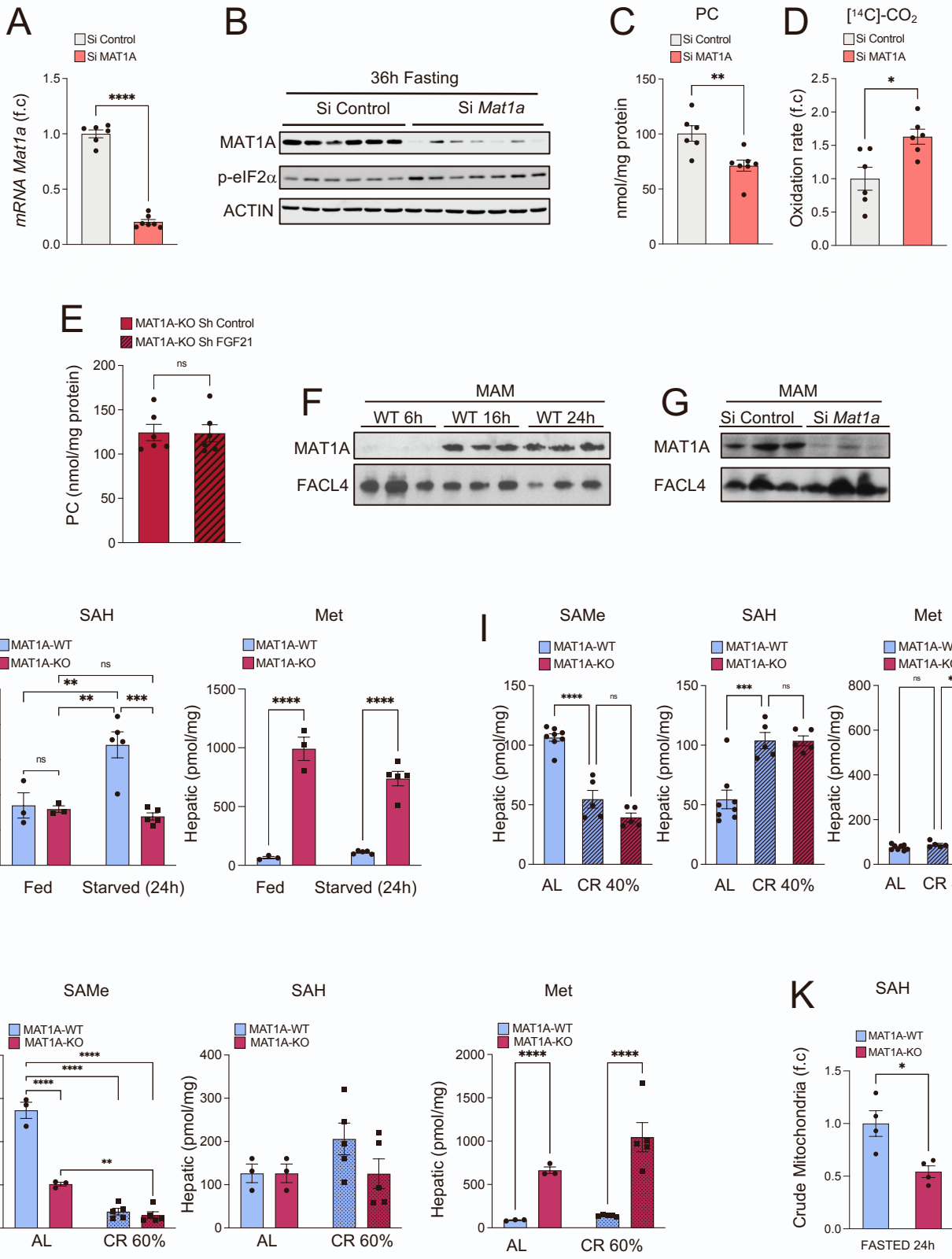

Supplemmetary Figure 4

Figure S4. ***Hepatic MAT1A during fasting is required to modulate β-oxidation, PC synthesis and ERS, related to Figure 5 and 6.***

(**A**-**E**) Hepatic *Mat1a* was acutely silenced in 3-month-old C57BL/6 mice by tail vein injection using specific siRNA (at time -24 and 0h), and then mice were subjected to a period of 36h of fasting (n=6-7 per group). (**A**) RT-qPCR of hepatic *Mat1a* gene showing strong reduction after silencing in these mice (n=6-7), (**B**) Immunoblot analysis of MAT1A and p-eIF2α in total liver extracts from *Mat1a*-silenced mice fasted during 36h (n=6). (**C**) Graph showing PC levels in livers from 36h-fasted control and *Mat1a*-silenced mice (n=6-7). (**D**) Hepatic fatty acid (palmitate) oxidation evaluated by measuring the release of radioactive [^{14}C]-CO_2 in livers from control and *Mat1a*-silenced mice fasted during 36h (n=6). (**E**) hepatic PC levels in total liver extracts in 36h-fasted MAT1A-KO mice after silencing of FGF21 (n=6). (**F**) Immunoblotting analyses from MAMs isolated from livers of C57BL/6 mice over a 6h, 16h and 24h period of fasting (n=3). (**G**) Immunoblot analysis showing strong downregulation of MATa1 in MAMs from livers of 36h-fasted *Mat1a*-silenced mice (n=3). FACL4 is used as loading control for MAMs. (**H**-**K**) UPLC analysis of (**H**) SAH and Met in total liver extracts from fed and fasted WT and MAT1A-KO mice (n=3-5), of (**I,J**) SAMe, Met and SAH in total liver extracts from WT and MAT1A-KO mice (**I**) fed during 2 months with 40% of CR (n=5-8) or (**J**) fed during 5 days with 60% of CR (n=3-5) (note that, SAMe, Met and SAH levels from livers of WT mice are from data shown in Figure 1B), of (**K**) SAH in crude mitochondrial extracts from 24h-fasted WT and MAT1A-KO mice (n=4). Results are presented as mean ± SEM. *p<0.05, ** p<0.01 and *** p<0.001 by two-way Anova (H-J) or Student's *t*-test (A, C, D, E and K). f.c. denoted fold change.

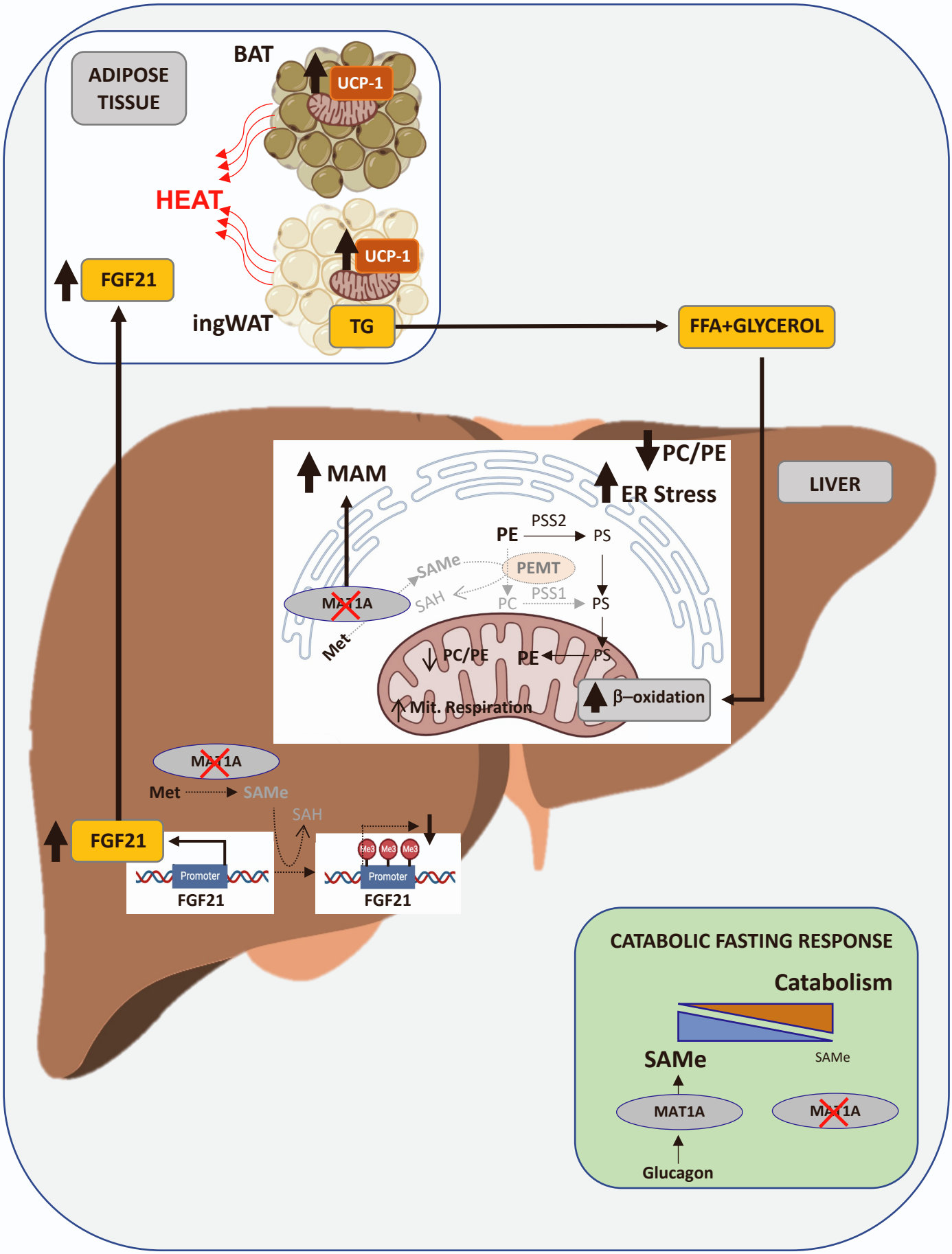

Supplemetary Figure 5

Figure S5. ***Model of action of SAMe as a metabolic sensor of nutritional restriction, related to Figures 1-6.***

A physiological reduction in hepatic SAMe levels induced by either food deprivation/restriction is associated with an enhancement of the activation of ER-mitochondria tethering and β-oxidation in the liver. This effect is remarkably phenocopied in mice with genetic ablation of *Mat1a*, which are characterized by a chronic reduction in SAMe levels, even under fed condition. At the same time, during these nutritional stresses, glucagon induces synthesis of MAT1A, which is then compartmentalized at MAMs, likely to produce SAMe locally that sustains PEMT activity and maintains the PC/PE ratio. This acts as a brake to prevent excessive hepatic β-oxidation, ATP production and ER stress, which ultimately prevents liver damage. In support of this mechanism, we show that blocking this local production of SAMe using mice lacking *Mat1a* removes this break leading to ERS and liver damage. At the systemic level, a chronic deficiency of SAMe levels induces lipolysis and browning of adipose tissue, likely due to an increased synthesis of the lipolytic factor FGF21 by the liver, induced by a reduction in CpG methylation in its promoter. In summary, a sustained decrease in hepatic SAMe levels could operate as a metabolic sensor of nutritional restriction to induce the catabolic lipid response, and maintenance of minimal SAMe synthesis at specific compartments such as MAMs could be essential for fine-tuning the catabolic response and preventing liver damage during fasting.

Table S1. Specifications of the primer sequences used, Related to STAR Methods.

Gene name	*Symbol*		Sequence
Adipose triglyceride lipase	*Atgl*	Forward primer	5´-GGTTAGAGTTGCTCAGCCGT-3´
		Reverse primer	5´- ACATGAGGAGCGGATGTGTG-3´
Fatty acid synthase	*Fas*	Forward primer	5´-GGCCCCTCTGTTAATTGGCT-3´
		Reverse primer	5´-GGATCTCAGGGTTGGGGTTG-3´
Fibroblast growth factor 21	*Fgf21*	Forward primer	5'-CTGCTGGGGGTCTACCAAG-3'
		Reverse primer	5'-CTGCGCCTACCACTGTTCC-3'
Glyceraldehyde-3-phosphate dehydrogenase	*Gapdh*	Forward primer	5'-TTGATGGCAACAATCTCCAC-3'
		Reverse primer	5'-CGTCCCGTAGACAAAATGG-3'
Hormone-sensitive lipase	*Hsl*	Forward primer	5´- TGAGATGGTAACTGTGAGCC-3´
		Reverse primer	5´-ACTGAGATTGAGGTGCTGTC-3´
Hypoxanthine guanine phosphoribosyl transferase	*Hprt*	Forward primer	5'-AAGCTTGCTGGTGAAAAGGA-3'
		Reverse primer	5'-TTGCGCTCATCTTAGGCTTT-3'
Hypoxanthine guanine phosphoribosyl transferase	*Hprt*	Forward primer	5'-AAGCTTGCTGGTGAAAAGGA-3'
		Reverse primer	5'-TTGCGCTCATCTTAGGCTTT-3'
Methionine adenosyltransferase 1A	*Mat1a*	Forward primer	5'-CCTCCCCCTACAAACCCAAC-3'
		Reverse primer	5'-CCGCTATCTCCCTCTTTGCC-3'
Monoacylglycerol lipase	*Mgl*	Forward primer	5´-GTTTGCCTGGCGCTGATACT-3
		Reverse primer	5´-GGGGTCTTTAGGCCCTGTTTC-3´
Phosphatidylethanolamine N-methyltransferase	*Pemt*	Forward primer	5´-ACTCATGCATGCTAGTCCCA-3´
		Reverse primer	5´-AGCAGTGAAGGGCTCTTCAT-3´
Sterol regulatory element-binding protein	*Srebp*	Forward primer	5´-GAGGCCAAGCTTTGGACCTGG-3´
		Reverse primer	5´-CCTGCCTTCAGGCTTCTCAGG-3´
Ribosomal RNA, 18S	*18S*	Forward primer	5´-GCACCACCACCCACGGAATCG-3´
		Reverse primer	5´-TTGACGGAAGGGCACCACCAG-3´
Uncoupling protein 1	*Ucp1*	Forward primer	5'-CACGGGGACCTACAATGCTT-3'
		Reverse primer	5'-ACAGTAAATGGCAGGGGACG-3'